

Comparison between strip and rib SOI microwaveguides for intra-chip light distribution

L. Vivien ^{a,*}, F. Grillot ^a, E. Cassan ^a, D. Pascal ^a, S. Lardenois ^a, A. Lupu ^a, S. Laval ^a,
M. Heitzmann ^b, J.-M. Fédéli ^b

^a *Institut d'Electronique Fondamentale, Université Paris Sud, CNRS UMR 8622, Bat. 220, 91405 Orsay Cedex, France*

^b *CEA-DRTILETI, 17 rue des Martyrs, 38054 Grenoble Cedex 9, France*

Available online 12 October 2004

Abstract

A comparative analysis of the strip and rib geometries guided wave devices (waveguides, bends, mirrors, beam splitters) is performed to realize an optical distribution to several outputs. For the strip structures, the optical losses are strongly sensitive to sidewall roughness due to processing, whereas for slightly etched submicron rib waveguides, optical losses are lower than 0.4 dB/cm. The design, realization and characterization of an H-tree optical distribution from one input to 16 output points using 1 cm long rib waveguides, four compact T-splitters and two mirrors are presented. A 2.6 μ W optical power is obtained at each output for a 3 mW input power. This corresponds to an excess loss of 14 dB which seems to be sufficient for an integrated photodetector.
© 2004 Elsevier B.V. All rights reserved.

1. Introduction

The increase of integrated circuit complexity leads to a growing difficulty in designing large scale chips. CMOS technology will meet severe bottlenecks in particular due to global interconnect performance limitation. As mentioned in the International Technology Roadmap for Semiconductors (ITRS) [1], a promising solution comes from the use of optical interconnects which could allow a further increase of clock frequency [2]. Optical clock signal distribution from one input to several monolithically integrated photodetectors is considered to overcome the bottleneck of metallic interconnects using a compact SOI waveguide network on chip sizes larger than a few cm^2 . The on-chip clock distribution is based on the use of a monochromatic light source with an integrated modulator, an optical distribution made of passive components, and integrated photode-

tectors at each end of the tree branch. The passive network is formed by optical waveguides, splitters, and 90° turns [6].

The main advantages of optics are: large bandwidth, decreased power consumption, improved synchronization and immunity to electromagnetic noise and temperature changes.

The use of silicon on insulator (SOI) substrates to realize on-chip optical interconnects has the advantage of compatibility with existing CMOS technology. The large index difference between silicon and its oxide ($\Delta n = 2$) offers the potential for high-density optical component integration. The thin upper silicon film is transparent in the wavelength region at $\lambda \geq 1.1 \mu\text{m}$ and so can be used for the realization of optical waveguides. Strong light confinement waveguides are obtained by either partial etching of the silicon film leading to rib geometry [3], or by full etching of the silicon film down to the buried oxide to get strip geometry [4].

The highest compactness is realized with single-mode submicron strip waveguides exhibiting a negligible crosstalk between the nearest neighboring waveguides.

* Corresponding author. Tel.: +33 01 6915 4070; fax: +33 01 6915 4000.

E-mail address: laurent.vivien@ief.u-psud.fr (L. Vivien).

The performances of rib and strip structures are limited by the level of light scattering out of the plane mostly induced by side-wall roughness resulting from processing.

This article presents results for strip and rib SOI microwaveguides and discusses the possibility to use them for optical light distribution at the wavelength of $1.3\ \mu\text{m}$ over the chip area.

In Section 2, optical SOI structures such as couplers, waveguides, 90° -turns, splitters required to realize a passive H-tree optical distribution are described using either strip or rib structures.

Section 3 presents the experimental demonstration of an H-tree optical distribution from 1 input to 16 outputs using 1-cm long slightly etched submicron rib waveguides, four beam splitters and two mirrors.

2. Optical components

The particularity of SOI substrates used for micro-photonics applications in comparison with microelectronic ones is the relatively high buried silicon oxide layer thickness, necessary to avoid optical leakage towards the silicon substrate at the wavelength of $1.3\ \mu\text{m}$. The buried silicon oxide thickness has been chosen as $700\ \text{nm}$. The silicon film thicknesses are either of $380\ \text{nm}$ or $200\ \text{nm}$.

The optical loss measurements of the passive optical components are realized using grating couplers. The structures are inserted between two grating couplers, with linear transitions (1 mm long) from the gratings to the waveguide (Fig. 1a). The grating coupler size is $100\ \mu\text{m}$ long and $30\ \mu\text{m}$ wide to facilitate laser beam focusing at the input [3]. A Scanning Electron Microscope (SEM) view of a grating coupler is shown in Fig. 1b. The grating groove depths are $70\ \text{nm}$ or $30\ \text{nm}$, with a grating period of $430\ \text{nm}$ or $500\ \text{nm}$ for heights of $380\ \text{nm}$ or $200\ \text{nm}$, respectively, to couple the $1.3\ \mu\text{m}$ laser beam. This corresponds to incidence angles close to 10° to resonantly excite the TE propagation mode in the waveguide. A $700\ \text{nm}$ thick silica cladding is deposited onto the waveguide. These parameters have been chosen to insure high efficiency light coupling through a grating coupler [10].

The power P_{inj} injected into the waveguide is equal to $P_{\text{in}} - (P_{\text{r}} + P_{\text{t}})$ where P_{in} is the input power, while P_{r} and P_{t} are the reflected and the transmitted power part respectively. The grating coupler efficiency is given by $P_{\text{inj}}/P_{\text{in}}$. Average values of 55% for a $380\ \text{nm}$ height and 50% for a $200\ \text{nm}$ height have been measured.

After propagation in the passive structure, the guided wave is decoupled by an output grating on both sides of the chip (P_{dr} and P_{dt}). The total decoupled light power is given by $P_{\text{d}} = P_{\text{dr}} + P_{\text{dt}}$. In order to determine losses of each optical structure the ratio $P_{\text{d}}/P_{\text{in}}$ is measured.

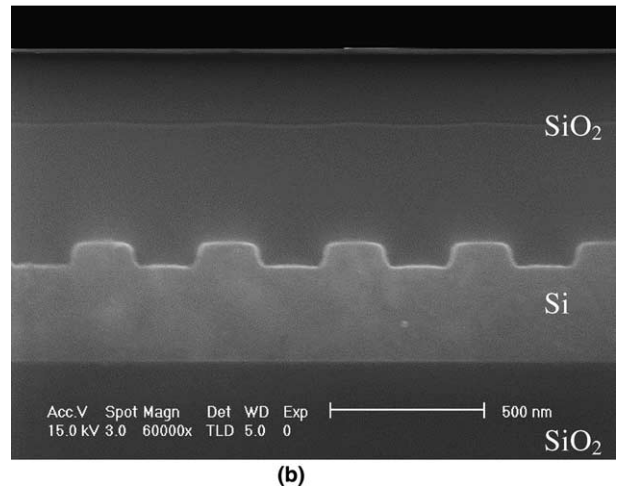
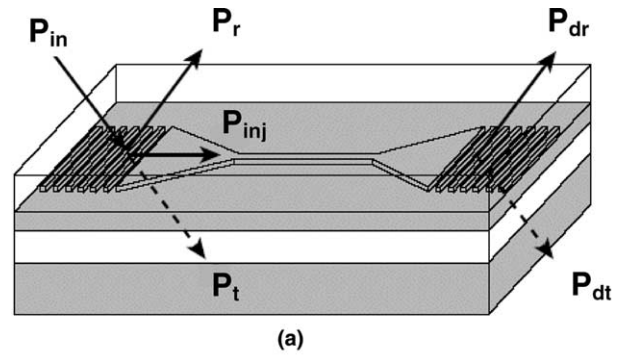


Fig. 1. (a) Schematic representation of the device for waveguide characterization: the waveguide is inserted between the input and output grating couplers via linear transition (a). (b) SEM view of grating coupler.

2.1. Strip SOI structures

Fig. 2a presents schematic view of strip SOI waveguides. Two kinds of strip waveguides have been realized and characterized. The first one is a square strip waveguide with a $380\ \text{nm}$ cross-section (type A) and the second is a rectangular waveguide with a $500\ \text{nm}$ width and a $380\ \text{nm}$ height (type B). Both strip waveguides exhibit a multimode behavior. In the case of a square cross-section below $320\ \text{nm}$, the single mode propagation is obtained [7]. For a width fixed to $500\ \text{nm}$, single-mode propagation is given for a height lower than $110\ \text{nm}$ at wavelength $1.3\ \mu\text{m}$. The advantage of using strip waveguides is the strong mode confinement [8], as shown by the simulation presented in Fig. 2b.

Propagation losses are measured with a method derived from the cutback one. Five straight strip waveguides with lengths ranging from 0.1 to $1\ \text{cm}$ are used. The normalized decoupled power is plotted in Fig. 3 as a function of waveguide lengths for both strip waveguides. In the case of structures A and B, the insertion losses are $4.2 \pm 0.8\ \text{dB}$ (Fig. 3a) and of $3 \pm 0.8\ \text{dB}$

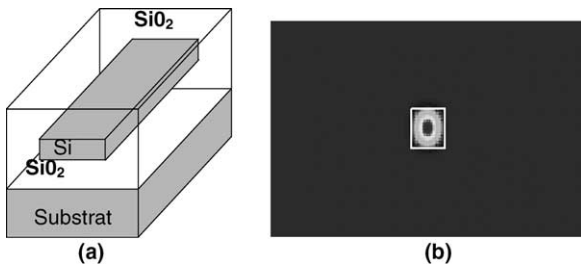


Fig. 2. Schematic view of (a) a strip waveguide and (b) the mode profile intensity.

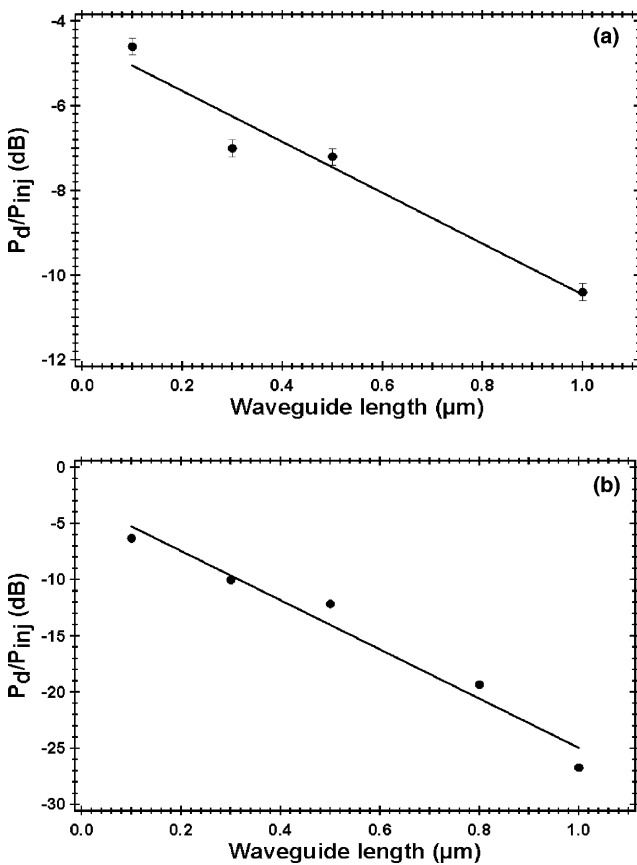


Fig. 3. Optical loss as a function of waveguide length. (a) Strip waveguide: 500nm wide and 200nm height. (b) Strip waveguide: 380nm wide and 380nm height.

(Fig. 3b), respectively. The propagation losses are 6.4 ± 1.4 dB/cm for the $500\text{nm} \times 380\text{nm}$ cross-section (Fig. 3a). They are much higher (22 ± 2 dB/cm) in the case of 380nm square cross-section waveguides (Fig. 3b). These propagation losses are mainly caused by strong light scattering on the side-wall roughness related to the processing [4,5]. Scattering on the side-wall roughness depends strongly on the confinement factor of the optical mode and the guiding geometry. Lower scattering losses can be obtained when the contrast between the optical mode effective index and the outside waveguide region refractive index decreases [5]. Recent works

have demonstrated lower propagation losses, below 4dB/cm for strip waveguides (200nm height and 500nm width) of comparable size [13,14]. This optical loss difference is due to a lower sidewall roughness.

For strip waveguides, 90° -bends with a few micron radii display low loss due to the strong light confinement [12,16]. Fig. 4 shows a 3D-Finite Difference Time Domain simulation (FDTD) [17] and a SEM view of a 90° -bend with a radius of $4\mu\text{m}$ in a square waveguide. Theoretical optical losses are about 0.08 dB for a $4\mu\text{m}$ bend at a wavelength of $1.55\mu\text{m}$.

For beam splitter, recent work has been published concerning T-branches optimized for strip waveguides with theoretical and experimental excess losses of 0.5dB and 1.5dB, respectively [12].

The optical losses obtained under this study for strip waveguides are too high to use such waveguides for optical signal distribution from one input to several output points over a whole microelectronic chip (which has a typical size of several cm^2). However, considering the best works on strip devices (propagation, 90° turns and beam splitters), the use of strip structures for optical interconnect applications is possible.

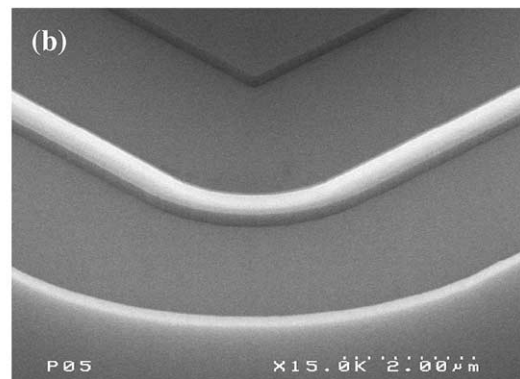
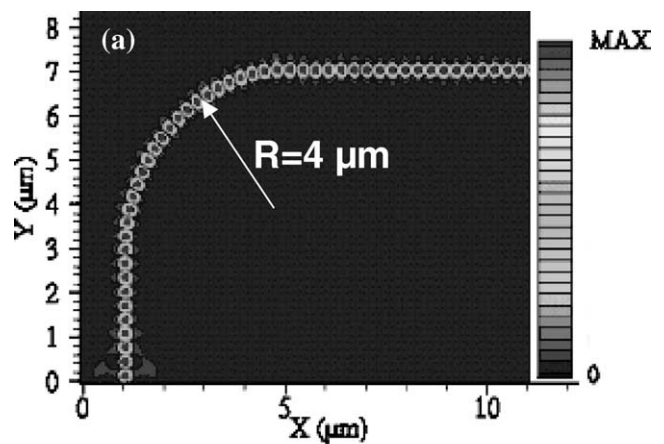


Fig. 4. (a) 3D-FDTD simulation and (b) SEM view of 90° -bend with a curvature radius of $4\mu\text{m}$ using submicron square strip waveguide.

2.2. Rib SOI waveguides

The width of rib waveguides is fixed at $1\mu\text{m}$. The etching depths are either 70nm for 380nm height (type C) or 30nm for 200nm height (type D). The C type waveguides exhibit single-mode propagation [3,9], while D types are multimodes. A schematic view of a slightly etched submicron rib waveguide is represented in Fig. 5a. As shown in Fig. 5b, slightly etched submicron rib waveguides also provide a high degree of compactness.

The insertion losses due to both input and output transitions of C and D types are $0.6 \pm 0.5\text{dB}$ (Fig. 6a) and $0.8 \pm 0.3\text{dB}$ (Fig. 6b), respectively. The propagation

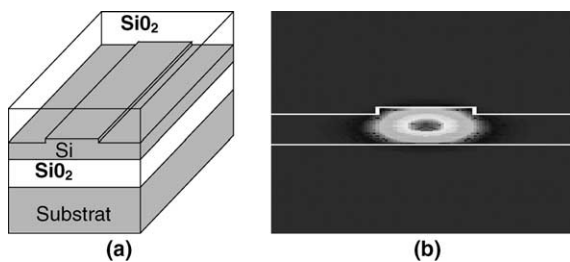


Fig. 5. Schematic view of (a) a slightly etched submicron rib waveguide and (b) the mode profile intensity.

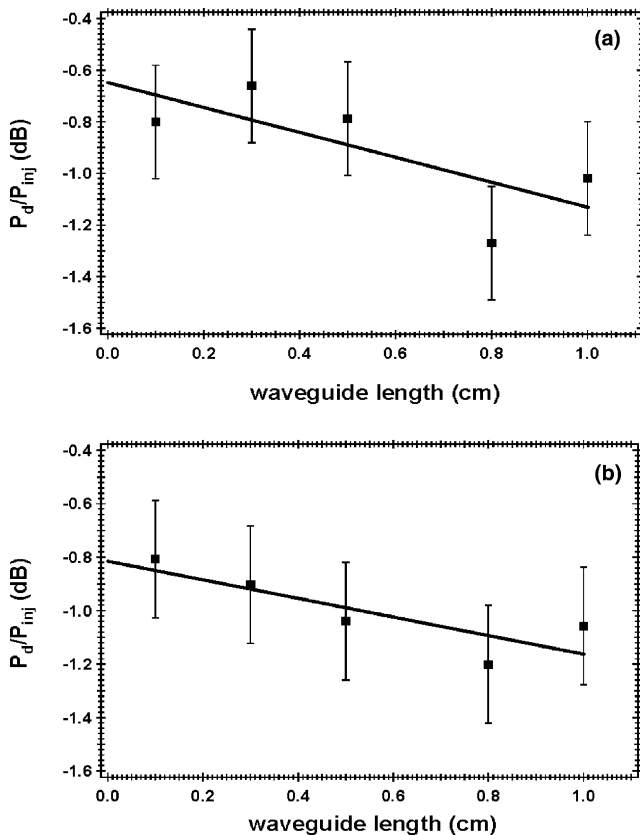


Fig. 6. Optical loss as a function of waveguide length. (a) Rib waveguide: $1\mu\text{m}$ wide, 380nm height and etch depth of 70nm . (b) Rib waveguide: $1\mu\text{m}$ wide, 200nm height and etch depth of 30nm .

optical losses are $0.4 \pm 0.3\text{dB/cm}$ (Fig. 6a) and $0.5 \pm 0.4\text{dB/cm}$ (Fig. 6b) for C and D types, respectively. The optical losses are lower for rib waveguides than for strip ones. Indeed, the mode intensity of the rib waveguide (Fig. 5) is lower in the vicinity of the etched surface compared to that in a strip waveguide (Fig. 2).

Rib waveguides exhibit a lower light confinement by comparison with strip guides. Therefore, due to the light leakage into a SiO_2 /partially-etched Si film/ SiO_2 slab waveguide, 90° -bends based on rib SOI waveguides usually require high curvature radii to minimize losses ($>50\mu\text{m}$). Then, fully etched corner mirrors are used with slightly-etched rib waveguides. 2D-FDTD simulation gives the light intensity repartition in the structure and a loss of about 0.1dB is achieved (Fig. 7a). A SEM view of the tested mirror is shown in Fig. 7b. The measured reflection losses are about 1dB and 0.9dB for 380nm and 200nm waveguide thicknesses, respectively.

As 1×2 splitters are required to perform distribution of optical signal, MultiMode Interferences (MMI) [15] and T-compact splitters (Fig. 8) [6,11] can be considered. Concerning the 1×2 MMI splitters, whose dimensions are typically $100\mu\text{m}$ long by $10\mu\text{m}$ wide for a slightly etched submicron rib geometry, experimental excess losses do not exceed 0.75dB for each branch.

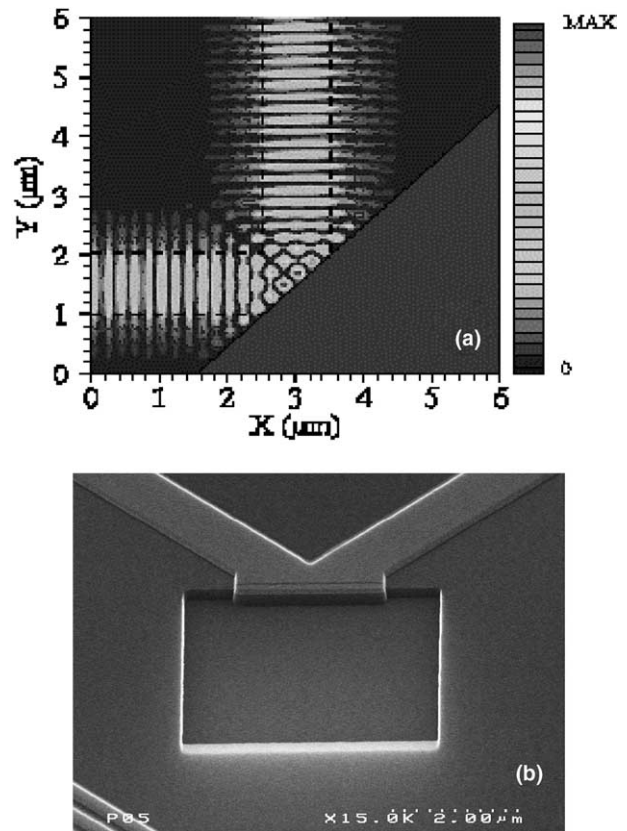


Fig. 7. (a) 2D-FDTD simulation and (b) SEM view of a corner mirror using rib waveguide.

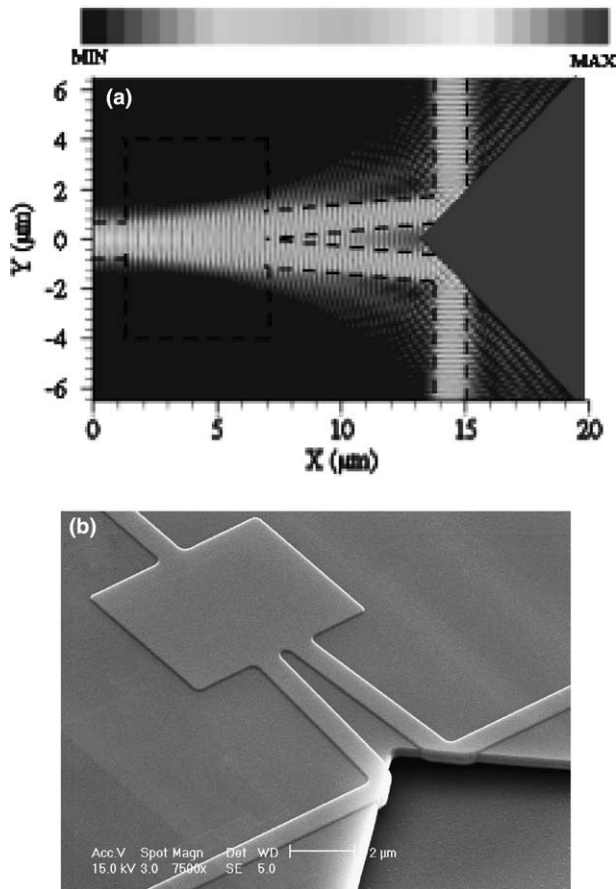


Fig. 8. (a) 3D-FDTD simulation and (b) SEM view of compact T-splitter using rib waveguides.

However, the MMI splitters are quite sensitive to temperature and process variations. These drawbacks are strongly penalizing for integration on a microelectronic chip. In order to improve device integration, a new ultra-compact T-splitter has been realized for rib geometry (Fig. 8b) [6,11]. The T-splitter was optimized for 380 nm thick SOI waveguides. It occupies an area of $8\mu\text{m}$ per $16\mu\text{m}$ and is much more compact than the MMI splitter. Fig. 8a shows a 3D-FDTD simulation of the T-splitter. The calculated excess losses are less than 0.3 dB at $1.31\mu\text{m}$ for each branch. Furthermore, a broadband efficiency ranging at least from $1.3\mu\text{m}$ to $1.6\mu\text{m}$ is obtained with temperature independence (Fig. 9).

The use of slightly etched submicron rib waveguides is a good compromise between high density integration and low optical loss.

3. Optical distribution

An H-tree optical distribution from 1 to 16 points has been realized using 200 nm thick rib waveguides. It has an unfolded length comparable to a chip size (about

1 cm) [18]. An optical microscope view of the distribution is shown in Fig. 9a. The laser beam is focused on the input grating coupler. The optical guided wave, after a 1 cm slightly etched submicron rib waveguide length with four compact T-splitters and 2 mirrors is decoupled at each output by similar grating couplers. Taking into account the optical loss of rib structures presented in Section 2.2, the global loss for each branch should be as low as 18.5 dB, assuming a rib waveguide loss of 0.5 dB/cm, a theoretical loss for the mirror of 0.2 dB and 0.5 dB for the T-splitter, a coupling efficiency of 50% (i.e. 3 dB) and an insertion loss of 0.6 dB. However, the total light power decoupled at the outputs has been measured and corresponds to an average power of -26 dB with respect to the input power. The optical loss difference is mostly due to higher losses for the various elements on this chip than for structures from another run as described above. The optical waveguide loss is 3.5 dB/cm, the T-splitter and mirror excess loss are estimated to be 2 dB and 1 dB, respectively, and the insertion loss is about 1 dB.

If a 3 mW input laser diode is used, a power of $2.6\mu\text{W}$ at each of the 16 outputs is obtained. This is roughly compatible with the minimum power required for an integrated photodetector to ensure a bit error rate (BER) of the order of 10^{-15} . Fig. 9b shows the 16 outputs observed with an infrared camera. All outputs are relatively well balanced ($\pm 0.7\text{ dB}$), excepted for two for which a variation lower than 5 dB is observed.

4. Conclusions

The use of strip and rib geometries has been investigated to distribute optical signal from one input to several outputs over a few centimeters. Concerning the strip geometry, the optical losses obtained for waveguides, splitters, and 90° -bends are strongly sensitive to side-wall roughness due to processing. The current state-of-art in terms of strip waveguide loss is higher than 2 dB for single-mode structures [13,14]. 90° -turns for strip geometry are realized using bends with a curvature radius of a few microns whose losses are below 0.1 dB [13]. The excess losses of compact splitters also depend strongly on side-wall roughness. The realization of an optical distribution to at least 16 output points using strip geometry is complicated because of the high degree of accuracy required on the technological process control to minimize scattering losses.

As a negligible crosstalk is achieved for a distance as small as $2\mu\text{m}$ between rib waveguides, this configuration does not much suffer from compactness by comparison with the strip one. Since optical losses are below 0.5 dB/cm, an H-tree optical distribution from one input to sixteen outputs has been realized, using four ultra-compact T-splitters, two mirrors, and 1-cm long rib

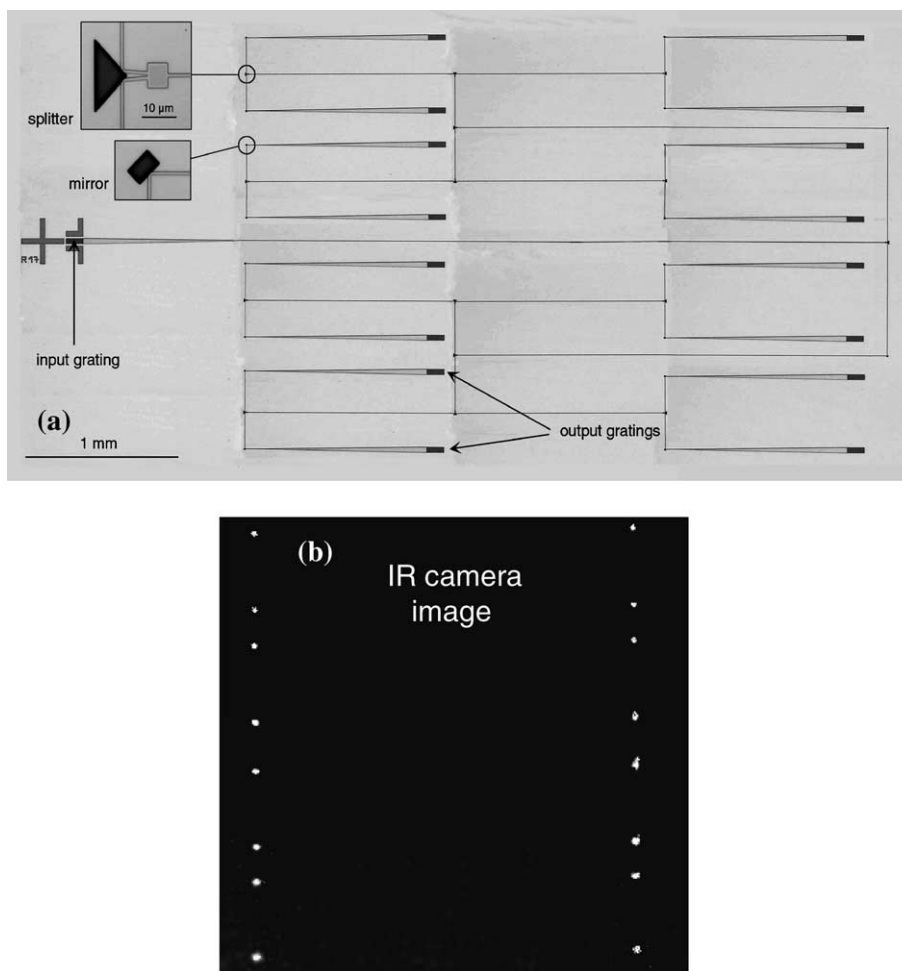


Fig. 9. (a) Optical microscopy view of the H-tree optical distribution from one input to 16 outputs. The T-splitter and corner mirror used are inserted in the left corner. (b) IR camera image of the 16 light outputs.

waveguides. Such a result is of prime importance since it constitutes the first successful experimental demonstration compatible with microelectronic chip sizes with -26 dB losses obtained at each output.

256 output points instead of 16 can be envisaged using the optimized rib structures presented in Section 2. Thus, slightly etched submicron rib waveguides are promising for the distribution of an optical signal to several points, combining compactness and very low loss. Further work will be devoted to monolithic integration of fast photodetectors at the end of each branch.

Acknowledgements

This work was supported by the French RMNT program “INOPCIS” in the frame of collaboration between Institut d’Électronique Fondamentale (CNRS/UPS Orsay), CEA-LETI (Grenoble), Laboratoire de Physique de la Matière (INSA Lyon), CNAM (Paris), and ST Microelectronics (Crolles). Authors acknowl-

edge Alain Koster from IEF and V. Le Goasoz from ST Microelectronics for fruitful discussions. They also acknowledge the staff of the 200 mm cleanroom of the LETI for the fabrication of high quality optical structures.

References

- [1] International Technology Roadmap for Semiconductors (ITRS), 2003 Edition, <http://public.itrs.net/>.
- [2] D.A.B. Miller, IEEE J. Selected Topics in Quant. Electron. 6 (2000) 1312.
- [3] S. Lardenois, D. Pascal, L. Vivien, E. Cassan, S. Laval, R. Orobtschouk, M. Heitzmann, N. Bouaida, L. Mollard, Opt. Lett. 28 (2003) 1150.
- [4] K.K. Lee, D.R. Lim, L.C. Kimerling, Optics Letters 26, vol. 23, pp. 1888–1890, 2001.
- [5] F. Grillot, L. Vivien, S. Laval, D. Pascal, E. Cassan, IEEE Phot. Techn. Lett. 16 (7) (2004) 1661.
- [6] E. Cassan, S. Laval, S. Lardenois, A. Koster, IEEE Journal of Selected Topics in Quantum Electronics 9 (2003) 460.
- [7] L. Vivien, S. Laval, B. Dumont, S. Lardenois, A. Koster, E. Cassan, Opt. Comm. 210 (2002) 43.

- [8] Photon Design corporation, FIMMWAVE, <http://www.photond.com>.
- [9] S. Lardenois, PhD Thesis n° 7319, Orsay (France), October 2003.
- [10] N. Landru, D. Pascal, A. Koster, *Opt. Comm.* 196 (2001) 139.
- [11] A. Koster, E. Cassan, S. Laval, L. Vivien, D. Pascal, *JOSA A*, in press.
- [12] R.U. Ahmad, F. Pizzuto, G.S. Camarda, R.L. Espinola, R.M. Osgood, *IEEE Phot. Techn. Lett.* 14 (2002) 65.
- [13] Yurii A. Vlasov, Sharee J. McNab, *Optics Express* 12 (2004) 1622.
- [14] W. Bogaerts, D. Taillaert, B. Luyssaert, P. Dumon, J. Van Campenhout, P. Bienstman, D. Van Thourhout, R. Baets, V. Wiaux, S. Beckx, *Optics Express* 12 (2004) 1583.
- [15] L.B. Soldano, E.C.M. Pennings, *J. Lightwave Technol.* 13 (1995) 615.
- [16] R.L. Espinola, R.U. Ahmad, F. Pizzuto, M.J. Steel, R.M. Osgood Jr., *Optics Express* 8 (2001) 517.
- [17] <http://www.ise.ch:EMLAB>.
- [18] L. Vivien, S. Lardenois, D. Pascal, S. Laval, E. Cassan, J.L. Cercus, A. Koster, J.M. Fédéli, M. Heitzmann, *Appl. Phys. Lett.* 85 (2004) 701.